View metadata, citation and similar papers at core.ac.uk
brought to you by CORE
provided by Institutional Repository of the Islamic University of Gaza

GUIDED MODES IN A METAL-CLAD WAVEGUIDE COMPRISING A LEFT-HANDED MATERIAL AS A GUIDING LAYER

Sofyan a. Taya[1] & Khitam Y. Elwasife[2]
[1,2] Physics Department, Islamic University Of Gaza, P.O. Box 108, Gaza, Palestinian Authority.
Email: Staya@Iugaza.Edu.Ps, Kelwasife@Iugaza.Edu.Ps

ABSTRACT
An investigation of guided modes supported by an asymmetrical three layer metal-clad waveguide structure is presented. A left-handed material (LHM) guiding layer sandwiched between a metal substrate and a dielectric cladding is considered. The dispersion characteristics of TE and TM polarizations are analyzed. The effect of the metal layer and the LHM parameters as well as the mode order on the dispersion characteristics and on the power flow is discussed in details. The results reveal many interesting properties for possible applications in optical waveguide sensing.

Keywords: *metal-clad waveguide, left-handed material*

1. INTRODUCTION

Optical waveguide structures play an important role in the field of optoelectronics. Among these structures, the metal-clad waveguide has found many applications in the active devices of optical circuit technology [1-3]. The attenuation of these metal-clad structures is, in general, relatively high but the energy lost by absorption in the metal region of a three-layered waveguide can be reduced by the addition of a thin dielectric layer between the dielectric core and the metal cladding. One of the most recent applications of metal-clad waveguides is as an optical waveguide sensor [4-6]. Salamon et al. [7,8] suggested a technique called coupled plasmon-waveguide resonance, in which a metal layer is introduced between the substrate and the guiding layer. This structure has lead to an improvement in the optical sensitivity of optical waveguide sensors.

The physical realization of materials with negative index of refraction was demonstrated recently for a novel class of engineered composite materials, now called left-handed materials (LHMs). Such materials have attracted attention not only due to their recent experimental realization and a number of unusual properties observed in experiment, but also due to the expanding debates on the use of a slab of a LHM. Pendry et al. analyzed principles of negative permittivity caused by metal strips array [9] and negative permeability caused by split-ring-resonators array [10] in theory, then Shelby et al. experimentally verified negative refractive index effect in these structures [11]. Since then much attention has been drawn to this type of metamaterial [12-16]. The dispersion properties of symmetric [14] and asymmetric [15] slab waveguides with LHM guiding layer have been studied in details. A slab waveguide with an anisotropic LHM core whose permittivity tensor is partially negative has been analyzed and some properties of the guided modes have been investigated [16].

The aim of the present work is to study analytically the propagation of electromagnetic waves in a metal-clad waveguide structure. A lossy LHM slab as a guiding layer is sandwiched between a semi-infinite metal as a substrate and a semi-infinite dielectric cladding. The dispersion relation is derived for both TE and TM waves. The power in each layer is presented. The effect of the metal layer and the LHM parameters on the propagation characteristics is examined in details.

2. MATHEMATICAL ANALYSIS

Geometry and notations for an asymmetric metal-clad waveguide structure under consideration is shown in Fig.1. We assume a guiding layer made of a LHM occupies the region $0 < z < h$ and bounded by a cladding and a metal substrate.

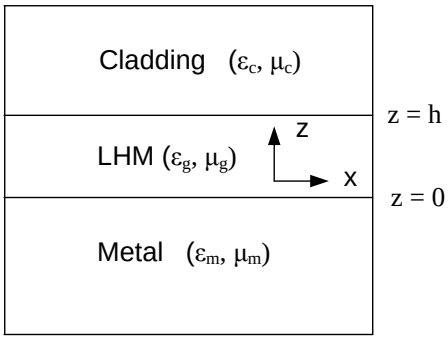

Figure 1. An asymmetric metal-clad waveguide with a LHM guiding layer.

The stationary solutions of the TE wave equation have the form $E_y(z)\exp(ik_x x - \omega t)$, where the amplitude $E_y(z)$ is real, k_x is the propagation constant along the longitudinal direction and ω is the frequency of the wave. Using this form of the stationary solution, Maxwell's equations can be written as

$$\frac{\partial^2 E_y(z)}{\partial z^2} + (k_0^2 \varepsilon_i \mu_i - k_x^2) E_y(z) = 0, \quad (1)$$

where k_0 is the free space wave number, $i = m$, g, or c indicating the metal, guiding layer or cladding, and $k_x = k_0 N$ with N is the modal index of the propagating mode.
In a similar manner, for TM we have

$$\frac{\partial^2 H_y(z)}{\partial z^2} + (k_0^2 \varepsilon_i \mu_i - k_x^2) H_y(z) = 0. \quad (2)$$

The solution of Eq. (1) in the three-layer structure is given by

$$\left.\begin{aligned} E_{y,c} &= A\exp(-k_{z,c}(z-h)),\ z>h \\ E_{y,g} &= B\exp(-ik_{z,g}z) + C\exp(ik_{z,g}z),\ 0<z<h \\ E_{y,s} &= D\exp(k_{z,s}z),\ z<0 \end{aligned}\right\}, \quad (3)$$

where $k_{z,c} = \sqrt{k_x^2 - k_0^2 \varepsilon_c \mu_c}$, $k_{z,g} = \sqrt{k_0^2 \varepsilon_g \mu_g - k_x^2}$ and $k_{z,m} = \sqrt{k_x^2 - k_0^2 \varepsilon_m \mu_m}$. The constants *A*, *B*, *C*, and *D* represent the amplitudes of the wave in the different layers.

The nonzero magnetic field components (H_x and H_z) of the TE modes can be calculated using $H_x = \frac{-k_0 N}{\omega \mu} E_y$ and $H_z = \frac{i}{\omega \mu}\frac{\partial E_y}{\partial x}$. From which we obtain

$$\left.\begin{aligned} H_{x,c} &= \frac{-ik_{z,c}}{\omega\mu_0\mu_c} A\exp(-k_{z,c}(z-h)),\ z>h \\ H_{x,g} &= \frac{k_{z,g}}{\omega\mu_0\mu_g} B\exp(-ik_{z,g}z) - \frac{k_{z,g}}{\omega\mu_0\mu_g} C\exp(ik_{z,g}z),\ h>z>0 \\ H_{x,m} &= \frac{-ik_{z,m}}{\omega\mu_0\mu_m} D\exp(k_{z,m}z),\ z<0 \end{aligned}\right\}, \quad (4)$$

and

$$\left.\begin{aligned} H_{z,c} &= \frac{k_x}{\omega\mu_0\mu_c} A\exp(-k_{z,c}(z-h)),\ z>\mathrm{h} \\ H_{z,g} &= \frac{k_x}{\omega\mu_0\mu_g} B\exp(-ik_{z,g}z) - \frac{k_x}{\omega\mu_0\mu_g} C\exp(ik_{z,g}z),\ 0<z<\mathrm{h} \\ H_{z,m} &= \frac{k_x}{\omega\mu_0\mu_m} D\exp(k_{z,m}z),\ z<0 \end{aligned}\right\}. \quad (5)$$

Matching the tangential electric and magnetic fields at z = 0 and z = h, the dispersion relation for TE modes is obtained

$$k_{z,g}h = \tan^{-1}\left(\frac{\mu_g}{\mu_m}\frac{k_{z,m}}{k_{z,g}}\right) + \tan^{-1}\left(\frac{\mu_g}{\mu_c}\frac{k_{z,c}}{k_{z,g}}\right) + m_1\pi, \quad (6)$$

where $m_1 = 0, 1, 2, \ldots$ is the mode order.

Similarly for TM modes, H_y is also given by

$$\left.\begin{aligned} H_{y,c} &= A\exp(-k_{z,c}(z-h)),\ z>h \\ H_{y,g} &= B\exp(-ik_{z,g}z) + C\exp(ik_{z,g}z),\ 0<z<h \\ H_{y,m} &= D\exp(k_{z,m}z),\ z<0 \end{aligned}\right\}. \quad (7)$$

If the nonzero electric field components are calculated using $E_z = \frac{-i}{\omega\varepsilon}\frac{\partial H_y}{\partial x}$ and $E_x = \frac{k_0 N}{\omega\varepsilon} H_y$ and the boundary condition are applied, the dispersion relation for TM modes is obtained as

$$k_{z,g}h = \tan^{-1}\left(\frac{\varepsilon_g}{\varepsilon_m}\frac{k_{z,m}}{k_{z,g}}\right) + \tan^{-1}\left(\frac{\varepsilon_g}{\varepsilon_c}\frac{k_{z,c}}{k_{z,g}}\right) + m_2\pi, \quad (8)$$

When the propagation constant k_x exceeds a critical value, $k_{z,g}$ becomes purely imaginary. In this case, we let $k_{z,g} = i\alpha$ and the dispersion relation becomes

$$-\alpha h = \tanh^{-1}\left(\frac{\mu_g}{\mu_m}\frac{k_{z,m}}{\alpha}\right) + \tanh\left(\frac{\mu_g}{\mu_c}\frac{k_{z,c}}{\alpha}\right), \quad (9)$$

for TE modes and

$$-\alpha h = \tanh^{-1}\left(\frac{\varepsilon_g}{\varepsilon_m}\frac{k_{z,m}}{\alpha}\right) + \tanh\left(\frac{\varepsilon_g}{\varepsilon_c}\frac{k_{z,c}}{\alpha}\right), \quad (10)$$

for TM modes.

It is very important to study the effect of the negative parameters on the power associated with the propagating mode in each layer. The energy flux per unit length for TE modes is given by

$$p_{total} = \frac{k_0 N}{2\omega}\int_{-\infty}^{\infty}\frac{|E_y|^2}{\mu}dz. \quad (11)$$

From which the following results can be obtained

$$p_c = \frac{-k_0 N}{4\omega\mu_c k_{z,c}}\left[\frac{\mu_c}{\mu_g}\left(\frac{\mu_m+\mu_g}{\mu_m-\mu_g}\right)\exp(-ik_{z,g}h) - \frac{\mu_c}{\mu_g}\exp(ik_{z,g}h)\right]^2, \quad (12)$$

$$p_g = \frac{ik_0 N}{4\omega\mu_g k_{z,g}}\left[(\frac{\mu_m+\mu_g}{\mu_m-\mu_g})^2 \mathrm{e}^{-2ik_{z,g}h} - \mathrm{e}^{2ik_{z,g}h} - (\frac{\mu_m+\mu_g}{\mu_m-\mu_g})^2 - 4hki\,(\frac{\mu_m+\mu_g}{\mu_m-\mu_g})+1\right], \quad (13)$$

$$p_m = \frac{k_0 N}{4\omega\mu_m k_{z,m}}[(\frac{\mu_m+\mu_g}{\mu_m-\mu_g})+1]^2. \quad (14)$$

In a similar manner, the energy flux per unit length for TM modes is given by

$$p_{total} = \frac{k_0 N}{2\omega}\int_{-\infty}^{\infty}\frac{|H_y|^2}{\varepsilon}dz\,, \quad (15)$$

$$p_c = \frac{-k_0 N}{4\omega\varepsilon_c k_{z,c}}[\frac{\varepsilon_c}{\varepsilon_g}(\frac{\varepsilon_m+\varepsilon_g}{\varepsilon_m-\varepsilon_g})\exp(-ik_{z,g}h) - \frac{\varepsilon_c}{\varepsilon_g}\exp(ik_{z,g}h)]^2, \quad (16)$$

$$p_g = \frac{ik_0 N}{4\omega\varepsilon_g k_{z,g}}\left[(\frac{\varepsilon_m+\varepsilon_g}{\varepsilon_m-\varepsilon_g})^2 \mathrm{e}^{-2ik_{z,g}h} - \mathrm{e}^{2ik_{z,g}h} - (\frac{\varepsilon_m+\varepsilon_g}{\varepsilon_m-\varepsilon_g})^2 - 4hki\,(\frac{\varepsilon_m+\varepsilon_g}{\varepsilon_m-\varepsilon_g})+1\right], \quad (17)$$

$$p_m = \frac{k_0 N}{4\omega\varepsilon_m k_{z,m}}[(\frac{\varepsilon_m+\varepsilon_g}{\varepsilon_m-\varepsilon_g})+1]^2. \quad (18)$$

3. RESULTS AND DISCUSSION

The dispersion relations for TE and TM are solved numerically to find the modal wave index *N* of the guided mode. We consider the cladding to be air of $\varepsilon_c = 1$ and $\mu_c = 1$ and the guiding layer to be a LHM with negative ε_g and μ_g. Lossless LHM only represents an ideal case which cannot be realized in the present designs. Therefore, in the present work we treat LHMs with ε_g and μ_g having the form $\varepsilon_g = \varepsilon_r + i\varepsilon_i$ and $\mu_g = \mu_r + i\mu_i$ with ε_r and μ_r are both negative. The metal is assumed to be silver with ε_m = -16+0.52i, and μ_m = 1. To investigate the behavior of the modal index and the power propagating into the waveguide structure under consideration, the thickness of the guiding layer is changed from 60 - 600 nm and these parameters are calculated and plotted with the thickness of the guiding layer for different ε_g and μ_g.

The variation of the modal index of silver-clad left-handed waveguide with the thickness of the guiding layer is presented in Fig. 2 and Fig. 3 for TE and TM guided modes, respectively. From these figures, we observe that the fundamental mode (m = 0) does not exist in the metal clad waveguide structure with LHM guiding layer. Higher modes (m > 0) exist and have many remarkable features. With the increase of the guiding layer thickness, the modal index of the modes (m = 1, 2, 3, …) increases and saturates at a specific value of the thickness. The thickness at which the modal index saturates is essentially dependent on the mode order. As the mode order increases this thickness noticeably increases. Moreover, the two figures reveal a substantial dependence of the modal index on the mode order. For a given thickness, the higher the mode order is the lower the modal index. The first mode (m = 1) behaves differently from these modes. The modal index decays with increasing the guiding layer thickness for TE_1 mode. Mode degeneracy appears in the silver-clad left-handed waveguide for TM_1 mode. Two different thicknesses correspond to the same modal index as seen in the inset of Fig. 3.

To investigate the effect of the guided light polarization on the modal index, a comparison between TE and TM modes is shown in Fig. 4. It is clear that for the same modal index a thicker LHM guiding layer is needed to support TM polarized guided wave.

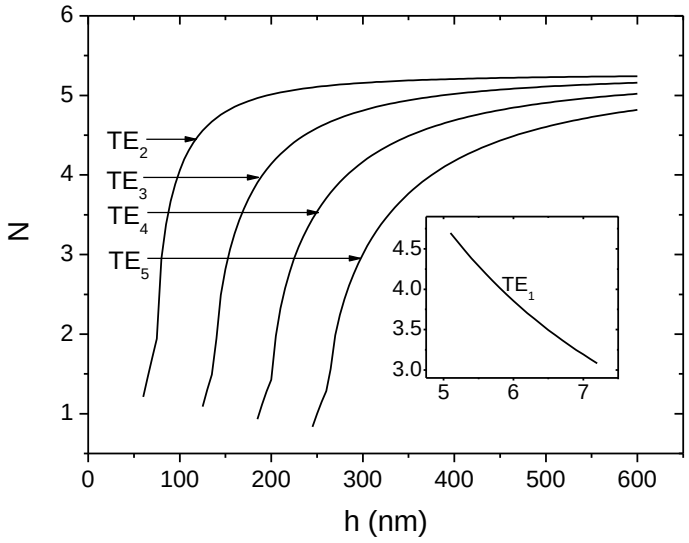

Figure 2. The modal index for TE guided modes of silver-clad left-handed waveguide when λ = 632.8 nm, ε_c = 1, μ_c = 1, ε_g = -3.7+0.001i, μ_g = -7.5+0.001i, ε_m = -16+0.52i, and μ_m = 1.

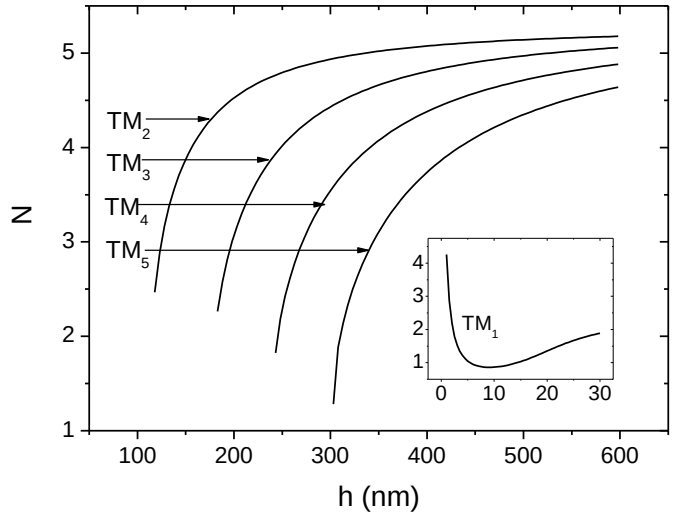

Figure 3. The modal index for TM guided modes of silver-clad left-handed waveguide when λ = 632.8 nm, ε_c = 1, μ_c = 1, ε_g = -3.7+0.001i, μ_g = -7.5+0.001i, ε_m = -16+0.52i, and μ_m = 1.

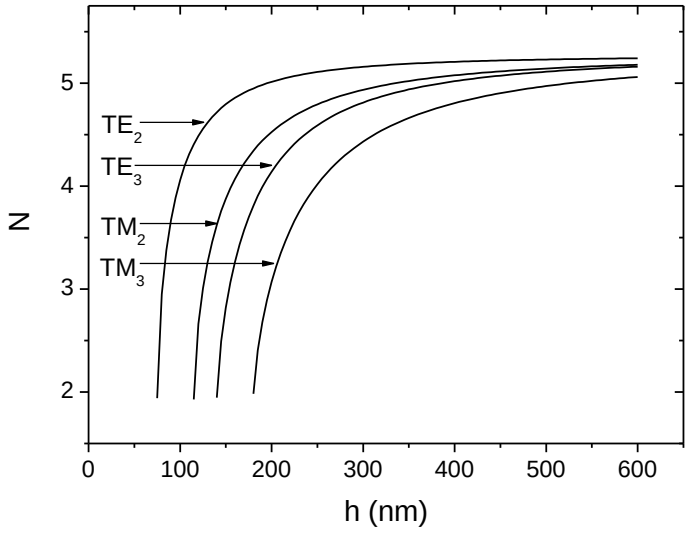

Figure 4. Comparison between TE and TM guided modes of silver-clad left-handed waveguide when λ = 632.8 nm, ε_c = 1, μ_c = 1, ε_g = -3.7+0.001i, μ_g = -7.5+0.001i, ε_m = -16+0.52i, and μ_m = 1.

A comparison between guided modes of silver-clad and gold-clad left-handed waveguide for both TE_2 and TM_2 modes is shown in Fig. 5. The effect of the metal layer on the modal index is not worth mentioning. As can be seen from the insets of the figure, a very slim decrease in the modal index occurs when the silver layer is replaced by gold one. Thus, the metal layer does not have a considerable effect when operating the proposed metal-clad waveguide in the guided mode configuration. However, the metal layer has a major effect when operating the structure in the reflection mode. In such a mode the waveguide is illuminated from below and we measure the reflectance from the waveguide as a function of the angle of incidence (θ_0). The reflectance from a layered structure can be calculated using Fresnel's reflection coefficients. For TE-mode, the reflectance from three-layer structure is given by

$$R_{123} = |r_{123}|^2 = \left| \frac{r_{sg} + r_{gc} \exp(2ik_{z,g}h)}{1 + r_{sg} r_{gc} \exp(2ik_{z,g}h)} \right|^2 , \tag{19}$$

$$r_{mg} = \frac{\mu_g k_{z,m} - \mu_m k_{z,g}}{\mu_g k_{z,m} + \mu_m k_{z,g}} , \; r_{gc} = \frac{\mu_c k_{z,g} - \mu_g k_{z,c}}{\mu_c k_{z,g} + \mu_g k_{z,c}} . \tag{20}$$

where r_{ij} is the reflection coefficient amplitude between layers *i* and *j*.

Figure 6 shows the reflectance as a function of the angle of incidence for TE wave reflected from silver-clad and gold-clad waveguide. The curves show a reflectance dip at which the reflectance minimizes. These dips are of high importance for optical waveguide sensors operated in reflected mode [17]. The position of the dip is crucially dependent on the metal layer. In the silver-clad structure, the dip occurs at $\theta_0 = 64.8^0$ whereas in the gold-clad structure it occurs at $\theta_0 = 76.2^0$.

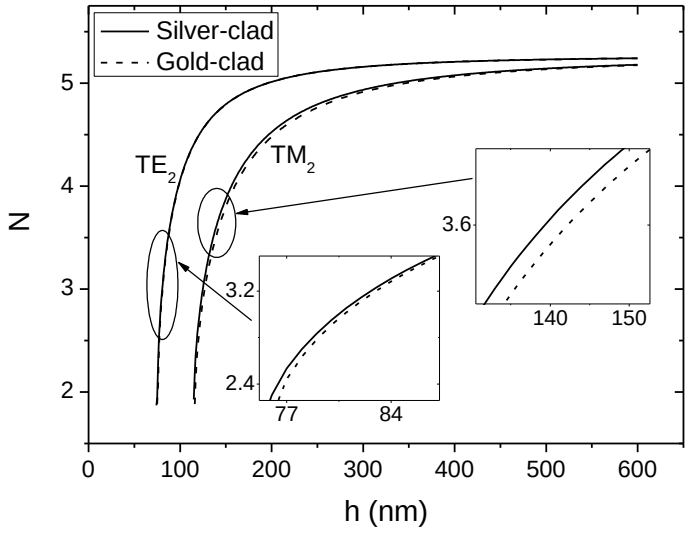

Figure 5. Comparison between guided modes of silver-clad and gold-clad left-handed waveguide for both TE_2 and TM_2 modes when $\lambda = 632.8$ nm, $\varepsilon_c = 1$, $\mu_c = 1$, $\varepsilon_g = -3.7+0.001i$, $\mu_g = -7.5+0.001i$, $\varepsilon_m = -16+0.52i$ (silver), $\varepsilon_m = -10.2+0.96i$ (gold) and $\mu_m = 1$.

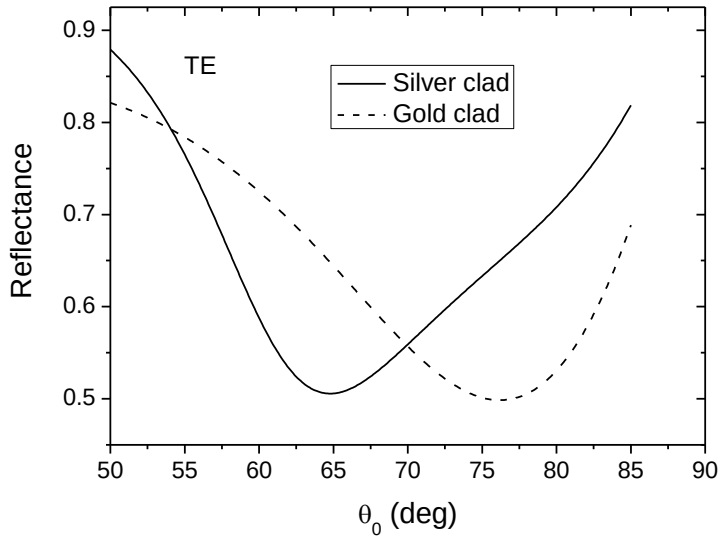

Figure 6. Reflectance as a function of the angle of incidence for TE wave reflected from silver-clad and gold-clad waveguide when $\lambda = 632.8$ nm, $\varepsilon_c = 1$, $\mu_c = 1$, $\varepsilon_g = -3.7+0.001i$, $\mu_g = -7.5+0.001i$, $\varepsilon_m = -16+0.52i$ (silver), $\varepsilon_m = -10.2+0.96i$ (gold) and $\mu_m = 1$.

It is very important when proposing a waveguide structure comprising a LHM layer to study the effect of the negative parameters of the LHM on the modal index of the guided mode. The modal index as a function of guiding layer thickness is shown in Fig. 7 for different values of the LHM permittivity for TE_2 mode and in Fig. 8 for TM_2 mode. In a similar manner, it is shown for different values of the LHM permeability for TE_2 and TM_2 modes in Fig. 9 and Fig. 10, respectively. The features that can be extracted from the figures is that for a given guiding layer thickness, the modal index of TE and TM modes is enhanced when the absolute value of the real part of the LHM

permittivity increases. The situation doesn't change when the absolute value of the real part of LHM permeability increases. For a given guiding layer thickness, the modal index of TE and TM modes is enhanced when either $|\mathrm{Re}(\varepsilon_g)|$ or $|\mathrm{Re}(\mu_g)|$ increases.

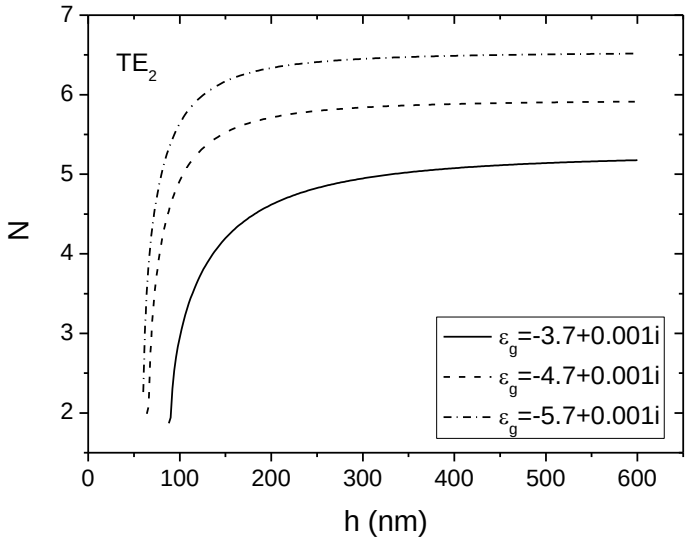

Figure 7. The modal index for TE guided modes of silver-clad left-handed waveguide for different values of ε_g when λ = 632.8 nm, ε_c = 1, μ_c = 1, μ_g = -7.5+0.001i, ε_m = -16+0.52i, and μ_m = 1.

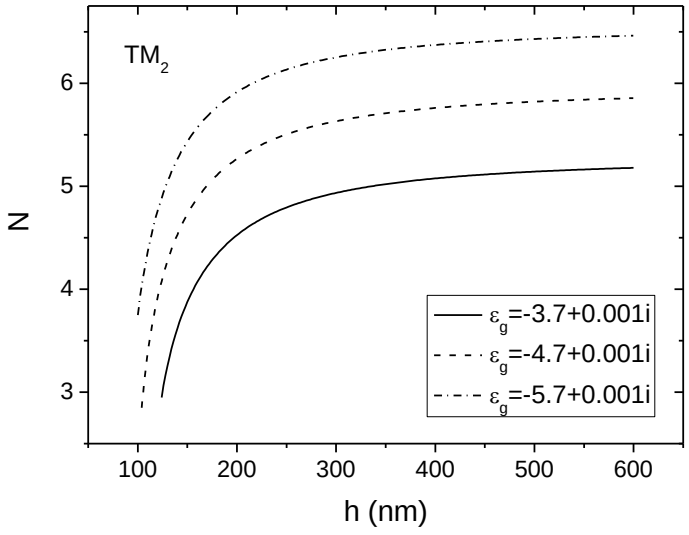

Figure 8. The modal index for TM guided modes of silver-clad left-handed waveguide for different values of ε_g when λ = 632.8 nm, ε_c = 1, μ_c = 1, μ_g = -7.5+0.001i, ε_m = -16+0.52i, and μ_m = 1.

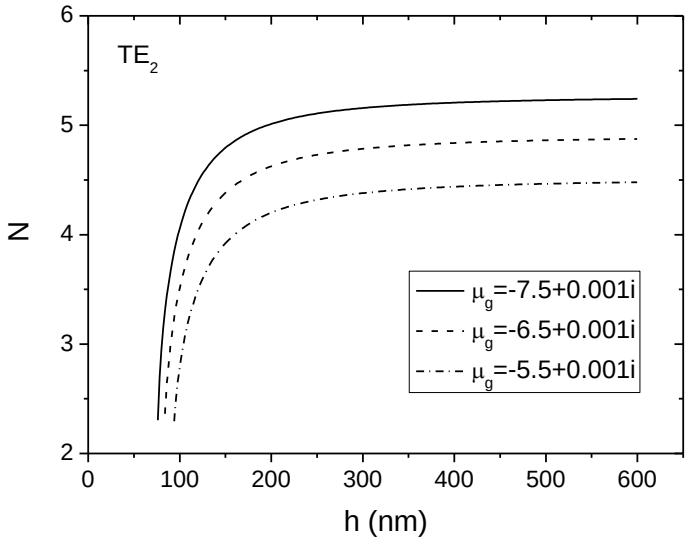

Figure 9. The modal index for TE guided modes of silver-clad left-handed waveguide for different values of μ_g when $\lambda = 632.8$ nm, $\varepsilon_c = 1$, $\mu_c = 1$, $\varepsilon_g = -3.7+0.001i$, $\varepsilon_m = -16+0.52i$, and $\mu_m = 1$.

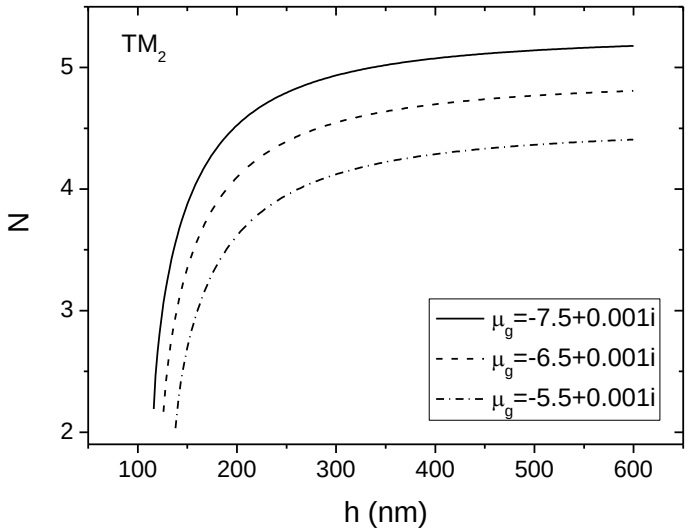

Figure10. The modal index for TM guided modes of silver-clad left-handed waveguide for different values of μ_g when $\lambda = 632.8$ nm, $\varepsilon_c = 1$, $\mu_c = 1$, $\varepsilon_g = -3.7+0.001i$, $\varepsilon_m = -16+0.52i$, and $\mu_m = 1$.

The power fraction flowing in each layer of a waveguide structure is considered one of the most determining criteria of the proper applications of the structure. When the power fraction of the guiding layer is high, this suggests applications requiring high wave confinement. On the other hand, when the cladding layer power is relatively high, we think about applications requiring large evanescent tail such as optical waveguide sensors operated in the guided mode configuration [18-25]. The sensing operation of such devices is performed by the evanescent tail of the modal field in the cover medium. The guided electromagnetic field of the waveguide mode extends as an evanescent field into the cladding and substrate media and senses a modal index of the guided mode. The modal index of the propagating mode depends on the structure parameters. As a result, any change in the refractive index of the

covering medium results in a change in the modal index of the guided mode. The basic sensing principle of the planar waveguide sensor is to measure the changes in the modal index due to changes in the refractive index of the covering medium.

The power flowing in the guiding layer as a function of the guiding layer thickness for different values of the real part of the LHM permittivity is shown in Fig. 11. Increasing the thickness of the guiding layer enhances the power flowing in it. This is a well known behavior since increasing the thickness of the guiding improves the wave confinement. Moreover, power flowing in the guiding layer can be enhanced by increasing the absolute value of the real part of LHM permittivity as well.

The dependence of the power flowing in the cladding layer on the guiding layer thickness for different values of the LHM permittivity is shown in Fig. 12 and for different values of the LHM permeability is shown in Fig. 13. The behavior of the power flowing in the cladding layer with the thickness is almost similar to its behavior in the conventional three layer waveguide structure [20-22]. The power flowing in the cladding has a sharp peak at a specific value of h, which we may recall the optimum value of h if the proposed metal-clad structure has been used as an optical waveguide sensor operated in the guided mode configuration. At this peak, the power flowing in the cladding layer and the sensitivity of the sensor are maximum. This peak is shifted toward lower values of h with increasing the absolute value of the LHM permittivity or the LHM permeability as shown in Fig. 12 and Fig. 13, respectively. Increasing the absolute value of the real part of the LHM permeability has another significant impact on the power flowing in the cladding. It causes the peak to diminish, thus reducing the sensitivity of the sensor. At small values of h near the cut-off, the power approaches zero since most of the total power flows in the substrate and the fraction of power flowing in the clad vanishes. To the right of this peak, we can see that the power in the cladding layer decreases as the core thickness gets thicker due to the high confinement of wave within the core layer.

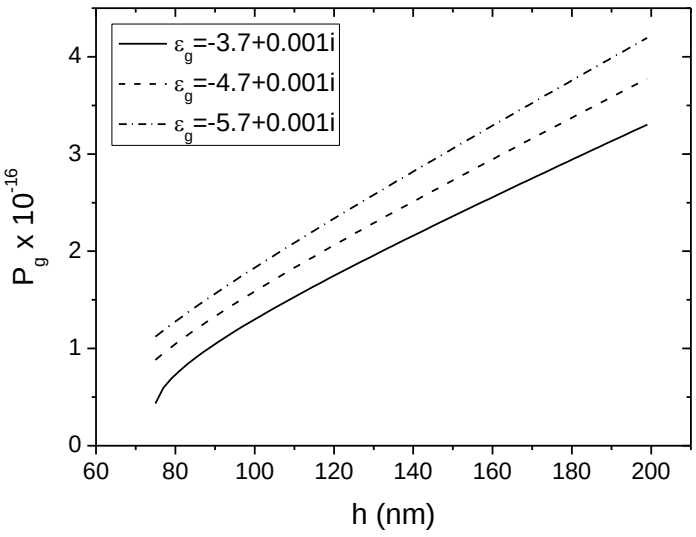

Figure 11. Power flowing in the guiding layer for TE guided modes of silver-clad left-handed waveguide for different values of ε_g when λ = 632.8 nm, ε_c = 1, μ_c = 1, μ_g = -7.5+0.001i, ε_m = -16+0.52i, and μ_m = 1.

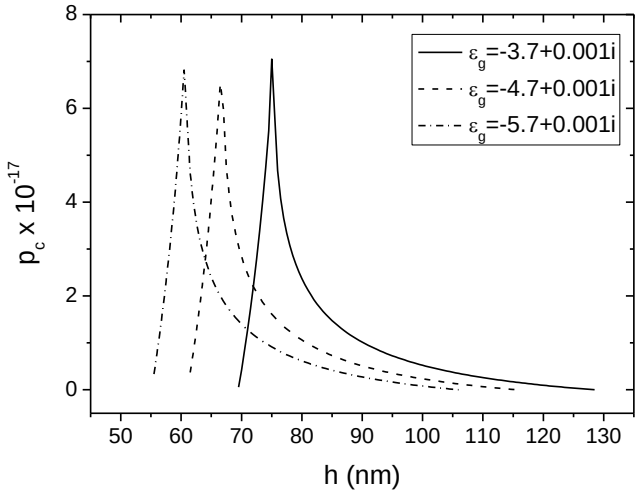

Figure12. Power flowing in the cladding layer for TE guided modes of silver-clad left-handed waveguide for different values of ε_g when λ = 632.8 nm, ε_c = 1, μ_c = 1, μ_g = -7.5+0.001i, ε_m = -16+0.52i, and μ_m = 1.

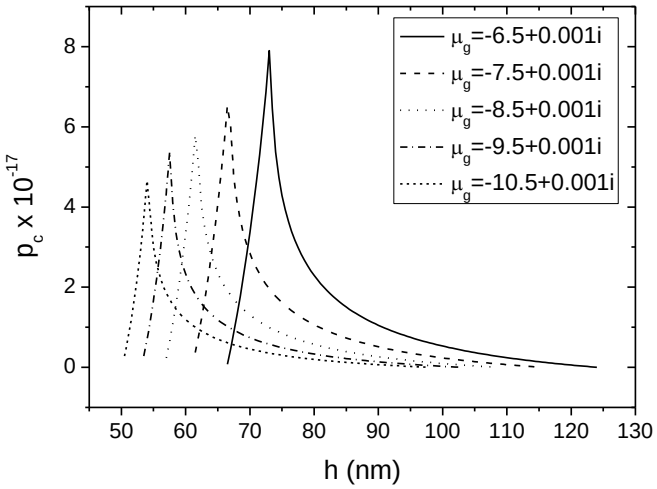

Figure 13. Power flowing in the cladding layer for TE guided modes of silver-clad left-handed waveguide for different values of μ_g when λ = 632.8 nm, ε_c = 1, μ_c = 1, ε_g = -3.7+0.001i, ε_m = -16+0.52i, and μ_m = 1.

4. CONCLUSION

Guided modes in an asymmetrical three layer metal-clad waveguide structure have been studied in details with a special focus on the effect of the metal layer and the LHM parameters on the dispersion characteristics and on the power flow. Many interesting features have been found. The fundamental mode does not exist in the proposed structure. The modal index of higher modes is essentially dependent on guiding layer thickness, the mode order, and the light polarization. The modal index is found to be enhanced when the absolute value of the real part of the LHM permittivity or permeability increases. A slight dependence of the modal index on the type of the metal used as a substrate has been observed when operating the proposed structure in the guided mode configuration whereas it has a major effect on the position of the reflectance dip when operating it in the reflection mode. The power flowing in the cladding is found to have a sharp peak at a specific value of the guiding layer thickness. The value of the power at this peak and the thickness at which it occurs are crucially dependent on the parameters of the LHM guiding layer.

5. REFERENCES

[1]. I.P. Kaminow, W.L. Mammal, H.P. Weber, Metal-clad optical waveguides: analytical and experimental study, Appl. Opt. 13, 396–405 (1974).

[2]. P.K. Tien, R.J. Martin, S. Riva-Sanseverino, Novel metal-clad optical components and method of isolating high-index substrates for forming integrated optical circuits, Appl. Phys. Lett. 27 , 251–253 (1975).

[3]. Y. Yamamoto, T. Kamiya, H. Yanai, Propagation characteristics of a partially metal-clad optical guide: metal-clad optical strip line, Appl. Opt. 14 ,1, 322–326 (1975).

[4]. C. Lee, Y. Jen, Influence of surface roughness on the calculation of optical constants of a metallic film by attenuated total reflection, Appl. Opt. 38 , 6029–6033 (1999).

[5]. M. Zourob, S. Mohr, B.J.T. Brown, P.R. Fielden, M. McDonnell, N.J. Goddard, The development of a metal clad waveguide sensor for the detection of particles, Sens. Actuators B 90 , 296–307 (2003).

[6]. M. Zourob, S. Mohr, P.R. Fielden, N.J. Goddard, Small-volume refractive index and fluorescence sensor for micro total analytical system (_-TAS) applications, Sens. Actuators B 94 , 304–312 (2003).

[7]. Z. Salamon, Y. Wang, G. Tollin, H.A. Macleod, Assembly and molecular organization of self-assembled lipid bilayers on solid substrates monitored by surface plasmon resonance spectroscopy, Biochim. Biophys. Acta 1195 , 267–275 (1994).

[8]. Z. Salamon, G. Tollin, Optical anisotropy in lipid bilayer membranes: coupled plasmon-waveguide resonance measurements of molecular orientation, polarizability, and shape, Biophys. J. 80 , 1557–1567 (2001).

[9]. J. B. Pendry, A. J. Holden, D. J. Robbins, W. J. Stewart, Low frequency plasmons in thin-wire structures, Phys. Condens. Matter. 10, 4785-4809 (1998).

[10]. J. B. Pendry, A. J. Holden, D. J. Robbins, W. J. Stewart, Magnetism from conductors and enhanced nonlinear phenomena, IEEE Tran. on Micr. Theo. and Tech. 47(11), 2075-2084 (1999).

[11]. R. A. Shelby, D. R. Smith, S. Schultz, Experimental verification of a negative index of refraction, Science. 292, 77-79 (2001).

[12]. Ying He , Zhuangqi Cao, Qishun Shen, Guided optical modes in asymmetric left-handed waveguides, Optics Communications . Vol. 245, No. 1-6, 125-135 (2005).

[13]. Slobodan M. Vuković, Najdan B. Aleksić, Dejan V. Timotijević ,Guided modes in left-handed waveguides, Optics Communications. Vol. 281, No. 6, 15, 1500-1509 (2008).

[14]. B.I. Wu, T.M. Grzegorczyk, Y. Zhang, and J.A. Kong, Guided modes with imaginary transverse wave number in a slab waveguide with negative permittivity and permeability, Journal of Applied Physics **93**, 9386–9388 (2003).

[15]. Y. He, Z. Cao, Q. Shen, Guided optical modes in asymmetric left-handed waveguides, Opt. Commun. 245 ,2005,pp. 125-135.

[16]. Guoan Zheng, Lixin Ran, "Light transmission along a slab waveguide with a core of anisotropic metamaterial, Optik 119 ,2008,pp. 591–595.

[17]. Skivesen N, Horvath R, Pedersen H. Optimization of metal-clad waveguide sensors. Sens. Actuators B 2005; 106:668-676.

[18]. Sofyan Taya, and Taher El-Agez, "Comparing optical sensing using slab waveguides and total internal reflection ellipsometry", Turkish J. of Physics, Vol. 35, 31-36, 2011.

[19]. Taher El-Agez and Sofyan Taya, "Theoretical spectroscopic scan of the sensitivity of asymmetric slab waveguide sensors ", Optica Applicata, Vol. 41, No. 1,2011,pp. 89-95, 2011.

[20]. Sofyan A. Taya, M.M. Shabat, H. Khalil, "Enhancement of Sensitivity in optical sensors using left-handed materials" Optik-International J. for Light and Electron Optics, vol. 120, 2009,pp. 504-508.

[21]. Sofyan A. Taya, M. M. Shabat, and H. Khalil, "Nonlinear Planar Asymmetrical Optical Waveguides for Sensing Applications", Optik-International J. for Light and Electron Optics, Optik-International J. for Light and Electron Optics, vol. 121, 2010,pp. 860-865.

[22]. M.M.Shabat, H. Khalil, Sofyan A. Taya, and M.M. Abadla, "Analysis of the sensitivity of self-focused nonlinear optical evanescent waveguide sensors", International Journal of Optomechatronics, vol. 1,2007,pp. 284-296.

[23]. Sofyan A. Taya and Taher M. El-Agez, "Reverse symmetry optical waveguide sensor using plasma substrate", J. of Optics, J. Opt. Vol. 13, 075701, 2011.

[24]. Sofyan A. Taya, Eman J. El-Farram, and Taher M. El-Agez, "Goos Hänchen shift as a probe in evanescent slab waveguide sensors", International Journal of Electronics and Communications, 2011, doi:10.1016/j.aeue.2011.07.004(In press),

[25]. Sofyan A. Taya and Taher M. El-Agez, "Optical sensors based on Fabry-Perot resonator and fringes of equal thickness structure", Optik - Int. J. Light Electron Opt., doi:10.1016/j.ijleo.2011.04.020 ,2011, (in press).